Constraint-Based Simulation for Non-Rigid Real-Time Registration

Hadrien Courtecuisse, Igor Peterlik, Raffaella Trivisonne, Christian Duriez, Stéphane Cotin

Constraint-Based Simulation for Non-Rigid Real-Time Registration

Hadrien COURTECUISSE [a,b] Igor PETERLIK [a] Raffaella TRIVISONNE [a,b]
Christian DURIEZ [b] Stéphane COTIN [a,b]
[a] *Institut Hospitalo-Universitaire, Strasbourg, France*
[b] *SHACRA Project, INRIA, France*

Abstract. In this paper we propose a method to address the problem of non-rigid registration in real-time. We use Lagrange multipliers and soft sliding constraints to combine data acquired from dynamic image sequence and a biomechanical model of the structure of interest. The biomechanical model plays a role of regularization to improve the robustness and the flexibility of the registration. We apply our method to a pre-operative 3D CT scan of a porcine liver that is registered to a sequence of 2D dynamic MRI slices during the respiratory motion. The finite element simulation provides a full 3D representation (including heterogeneities such as vessels, tumor, ...) of the anatomical structure in real-time.

Keywords. FEM, Non-Rigid Registration, Real-time, Lagrange multipliers

1. Introduction

Recent advances in the field of real-time simulation of deformable tissues may open the possibility to use simulations not only for training but also for pre and intra-operative support. Virtual simulations of anatomical structures could provide a strong support for the diagnostic phase, but also during the intervention in combination with augmented reality systems. Surgical simulations could result in significant decrease of risks for patients, and time/cost of the interventions. This is an important challenge in a context where a series of worldwide directives aims at optimizing the use of medical resources.

In this paper, our goal is to provide a full 3D model (including heterogeneities, tumors and vascular system...) of the liver during the respiration cycle. We acquired a pre-operative CT scan of a liver, and we aim at registering the segmented model to 2D dynamic slices acquired with MRI. We introduce a constraint-based method to couple a priori information provided a biomechanical model and intra-operative data obtained from image-based tracking of the surface of the liver in MRI slices.

2. Literature Review

2.1. Liver Motion and Deformable Registration

During the respiration cycle, the organs in abdominal cavity undergo important motion, mainly induced by the motion of diaphragm. In [13], the cranio-caudal translation is re-

ported as the dominant component of the liver motion during respiration (12–26 mm), compared to anterior-posterior (1–12 mm) and lateral (1–3 mm) motions. However, it is stated that purely rigid transformation is not sufficient to model the liver motion sufficiently during respiration, as some parts of the organ undergoes significant displacements (up to 35 mm) which cannot be captured with rigid registration.

The deformable registration is a well established area of research relying on biomechanical model of domain being registered. In the following we briefly survey relevant methods presented in the area of deformable registration, usually in context of preoperative planning and intra-operative guidance [3].

A 3D registration of intra-operative MR brain images is proposed in [5]: the model is based on linear elasticity discretized by the finite element method. The method is driven by active surface matching which deforms the boundary of brain in one acquired image towards the boundary in the following scan. The image warping based on finite element method is developed in [16]. The hyperelastic formulation is employed and the warping is applied in several domains, e.g. to measure strain in coronal artery or quantify morphology changes in mouse brain. A multi-organ deformable image registration based on mechanical model simulated with finite elements is developed in [2]. The model driven by surface deformation and displacements of landmarks is used to analyze and predict the motion of abdominal organ during respiration. Minimization of landmark displacements is used to drive the deformable registration of mouse brain in [8]: several regularization terms based on finite element formulation are compared including diffusion, linear and non-linear elasticity.

A technique based on Sum of Squared Differences (SSD) metric regularized with diffusion term applied to brain registration is presented in [12]. A geometrical mapping between the regular grid of image data and non-uniform FE mesh is presented, resulting in fast model-based image registration. In [9] preoperative 3D CT images are registered to either 3D or 2D intra-operative scans. While the registration is driven by optimization of similarity metrics (squared differences, mutual information and correlation ratio are considered), the mechanical model based on linear elasticity is used to regularize the solution. The method is tested on breast phantom. Multi-modality registration for image-guided prostate intervention is described in [7]: in the preoperative phase, a finite element patient specific model is built using the preoperative MR data and a set of deformations corresponding to different boundary conditions and randomly sampled material properties is computed and evaluated statistically using PCA. During the intervention, the ultrasound image is processed to extract the features and the likelihood is iteratively maximized resulting in warped MR data registered to the actual configuration of the prostate gland.

Liver deformation during respiration is studied in [11]. To address the issue a non-rigid registration framework relying on mesh-based inverse kinematics is presented. In [6], the biomechanical model of liver based on pre-operative CT images is used to estimate the actual position of a tumor based on tracking of surface features extracted from a laparoscopic camera during the intervention. Unlike our approach, elastic springs are used to provide a coupling between tracked features and the biomechanical model. In this paper, we introduce a constraint-based solution to allows the liver to “slide” along the control points defined by the outline of the liver. Our method allows robust non rigid registration and converges toward the configuration minimizing the amount of energy necessary to satisfy the constraints.

3. Methodology

3.1. Contour tracking and CT Semgentation

The model of the liver was constructed using contrast-enhanced CT data acquired on a female pig. The liver was segmented using semi-automatic methods available in ITKSnap[1] (see Fig. 1). A tetrahedral mesh was obtained from the segmented maps using CGAL[2]. Then a sequence of MRI slices was acquired (every 0.4175 second) in both coronal and sagittal axis, to capture the respiratory motion.

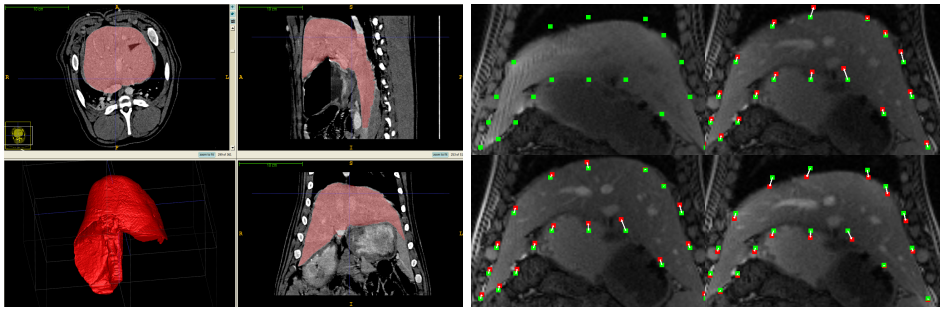

Figure 1. Data acquisition: (left) Semi automatic segmentation of a CT data acquired on a female pig using ITKSnap; (right) Contour tracking of the liver using optical flow algorithm. We manually defined a set of points (in green) located on the contour of the liver and we used OpenCV library to track the contour (in red) in the sequence of dynamic 2D MRI slices.

We manually defined a set of points on the boundary of the liver in the initial coronal and sagittal slices. These positions were tracked with an optical flow method available in OpenCV[3] (see Fig. 1). Knowing the position and orientation of the MRI slices, we obtain a set of sparse 3D control points that describe the motion (in the MRI plane) of the surface of the liver during the breathing cycles.

3.2. Simulation of Deformable Bodies

Finite Element Method (FEM) is best suited to handle material non-linearities as the constitutive law can be used explicitly. We use the corotational FEM introduced by [10]; while handling large displacements properly, it is restricted to small strain. In quasi static scenario, the governing differential equation at equilibrium for a time t is given by

$$f(\mathbf{q}_t) + \mathbf{B}(\dot{\mathbf{q}}_t) + \mathbf{f} + \mathbf{J}^T \lambda = 0 \tag{1}$$

where $\mathbf{f}$ are external forces (such as gravity), $f(\mathbf{q}_t)$ are the internal volumes forces at a given position $\mathbf{q}$ and $\mathbf{B}(\dot{\mathbf{q}}_t)$ a damping factor (obtained with Rayleigh damping). $\mathbf{J}^T$ and λ are respectively the Jacobian of the constraints and the associated constraint forces (see below) to register the model. At each time step, $f(\mathbf{q}_t)$ is evaluated with a first order linearization (see [1] for details):

[1] www.itksnap.org
[2] www.cgal.org
[3] http://opencv.org/

$$f_{\mathbf{q}_t} \approx f(\mathbf{q}_{t-1}) + \mathbf{K}(\mathbf{q}_{t-1})\, d\mathbf{q} \tag{2}$$

where $\mathbf{K}$ is the stiffness matrix that depends on the positions of the deformable body, and $d\mathbf{q} = \mathbf{q}_t - \mathbf{q}_{t-1}$ the difference of positions. Replacing (2) in (1) gives:

$$[-\mathbf{B}(\dot{\mathbf{q}}_t) - \mathbf{K}(\mathbf{q}_{t-1})]\; d\mathbf{q} \;=\; \mathbf{f} + f(\mathbf{q}_{t-1}) \;+ \mathbf{J}^T \lambda. \tag{3}$$

Defining δ as the initial interpenetration of the time step, $\mathbf{C} = (\frac{1}{h}\mathbf{B} + \mathbf{K})^{-1}$ the *compliance matrix* and $\mathbf{W} = \mathbf{JCJ}^{\mathrm{T}}$ the *Delassus operator*. λ can be obtained with the *Schur complement* method (see [4] for details) by solving the system

$$\mathbf{W}\lambda + \delta = 0. \tag{4}$$

3.3. Pairing Image Data and Simulation

Due to the plane motion, the control points provided by the MRI slices cannot be associated statically with the same material point in the liver. At each time step, the Iterative Closest Point (ICP) method [14] is used to bind the control points with their respective nearest triangle on the surface of the segmented liver. In Fig. 2(a) the control points (green) are associated (red lines) with the closer surface of the object (orange).

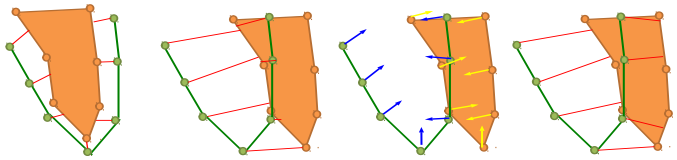

Figure 2. Binding process of the control points and the FE structure.

The method is improved by ensuring that the normals defined by the outline in the MRI sliced have the same orientation as the normals of the FE mesh. Indeed, in Fig. 2(b) the distance criterion is not sufficient since all the control points are associated with the same side of the object and the constraints cannot be satisfied. In Fig. 2(c), we define a set of normals aiming inside the liver, and in Fig. 2(d) the control points are associated with the closer triangle whose normal is oriented in the same direction.

3.4. Constraint-Based Registration

Using a proximity collision detection, the control points $\mathbf{q}_i$ are associated with their respective closer points $\mathbf{q}_s$ on the surface of the liver. The proximity information is reformulated on the Degrees of Freedom of the FE mesh using a mapping matrix $\mathbf{J}$ that links the positions from the contacts space to the motion space (see [15] for details):

$$\delta = dot(\mathbf{q}_i - \mathbf{J}\mathbf{q}_s, \mathbf{n}_c) \tag{5}$$

where δ is the violation of the constraints, and $\mathbf{n}_c$ is the normal of the nearest triangle.

At each time step a new paring procedure is called, and a single Lagrange multiplier is associated with each control point. Following [4], the constraint equations are solved (i.e. $\delta = 0$) at the end of each time step. As for the constraints in equation (5), $\mathbf{q}_s$ must be located on the tangential plane given by $\mathbf{n}_c$ at the end of the time step (see Fig. 3).

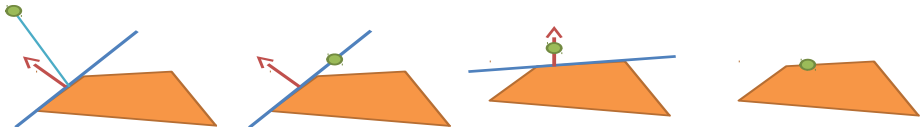

(a) Step 1 (begin) (b) Step 1 (end) (c) Step 2 (begin) (d) Step 2 (end))

Figure 3. At the end of each time step, the constraints are satisfied by simultaneously deforming the FE structure (orange) and moving the control points (green) along the tangential plane (blue) given by the normal (red) of the nearest triangle. 3(a), 3(b), 3(c) and 3(d) represent a configuration of two consecutive time step, respectively before and after the constraint resolution.

Image-based tracking methods still suffer from lack of accuracy and stability. Therefore, although the control points are expected to remain on the boundary of the liver, it is not always the case in practice.

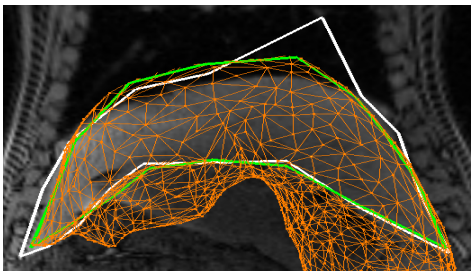

Figure 4. The white contour is directly given by image-based tracking where the top right control point has been intentionally displaced above the liver. The orange shape is the wireframe surface of the FE mesh and the green shape is the resulting polyhedron using soft constraints.

In order to improve the robustness of the method, a compliance factor is associated such that both the biomechanical model and the control outline can be deformed during the constraints resolution (see Fig. 4). Equation (4) is then replaced by:

$$(\mathbf{W} + \mathbf{W}^{\text{soft}})\,\lambda + \delta = 0 \tag{6}$$

where $\mathbf{W}^{\text{soft}}$ is a diagonal matrix whose coefficients are directly related to the confidence of the tracking method.

4. Results

We registered a preoperative CT scan acquired with MAGNETOM® Aera SIEMENS 1.5 T, to a sequence of 2D dynamic MRI slices acquired with a SOMATOM® Definition AS 128 slices. A sequence of 46 MRI slices was acquired (every 0.4175 second) in both

coronal and sagittal axis. We manually defined 18 and 12 points on the boundary of the organ in the initial coronal and sagittal slices. The resulting FE mesh was composed of $1,294$ nodes and $4,579$ linear tetrahedral elements (see Fig. 5).

The FE mesh was then initialized sufficiently close to the MRI data. Soft sliding constraints are defined between the FE mesh and the control points. The liver is rapidly re-oriented, deformed and stabilized towards the configuration minimizing the amount of energy necessary to satisfy the constraints. The virtual model follows the motion of the control points and provides a full 3D representation (including vessels) of the respiration cycles (see Fig. 5). Finally, the system is solved in real-time with an average framerate of 76 FPS (1 second is simulated in 0.65 second).

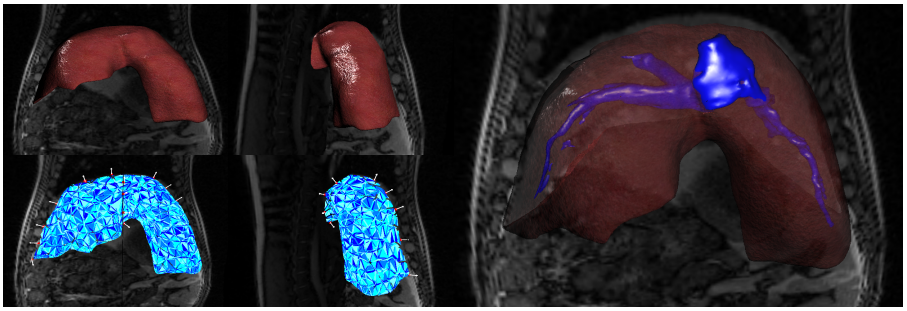

Figure 5. Full 3D registration of the liver CT preoperative scan to the sequence of 2D dynamic MRI slices. Large deformations and rotations are applied to the mesh , and the method remains stable and real-time during the breathing cycle.

A preliminary validation of our method was performed comparing the CT and MRI images as follows. First, the initial and deformed FE meshes were used to calculate the displacement field using the constraints driven by the contour extracted from a chosen MRI slice. Second, the displacement field was then used to warp the pre-operational CT volume. Finally, a slice corresponding to the location of the MRI aqusition plane was extracted from both the initial and warped CT data. The results presented in Fig. 6 show a good match between the target MRI and slice extracted from warped CT data, not only w.r.t. the overall shape of the liver, but also when comparing the positions of internal vascular structures.

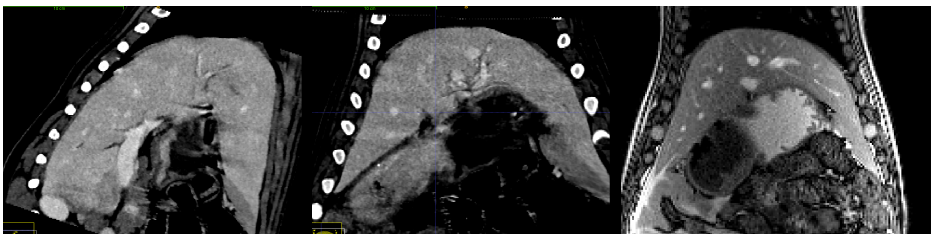

(a) Initial CT (b) Model-registed CT (c) Target MRI image

Figure 6. Preliminary validation: the initial CT data (a) are registered to target MRI (c) resulting in (b).

5. Conclusion

We proposed a method for non-rigid real-time registration. We combined advanced imaging techniques with a physics-based simulation to provide a 3D representation of the liver during the respiration motion. Our method relies on a generic constraint-based framework to solve both sliding and soft constraints. As future work we plan to incorporate anatomical landmarks constraints during the registration. The generic nature of our approach allows adding such constraints, which may be useful to avoid local minimum during the solving process.

References

[1] David Baraff. Linear-time dynamics using lagrange multipliers. In *Proceedings of SIGGRAPH 96*, pages 137–146. ACM, 1996.

[2] K. K. Brock, M. B. Sharpe, L. a. Dawson, S. M. Kim, and D. A. Jaffray. Accuracy of finite element model-based multi-organ deformable image registration. *Medical Physics*, 32(6):1647, 2005.

[3] Timothy J Carter, Maxime Sermesant, David M Cash, Dean C Barratt, Christine Tanner, and David J Hawkes. Application of soft tissue modelling to image-guided surgery. *Medical engineering & physics*, 27(10):893–909, December 2005.

[4] Christian Duriez, Frederic Dubois, Abderrahmane Kheddar, and Claude Andriot. Realistic haptic rendering of interacting deformable objects in virtual environments. *IEEE Transactions on Visualization and Computer Graphics*, 12(1):36–47, 2006.

[5] M Ferrant, a Nabavi, B Macq, F a Jolesz, R Kikinis, and S K Warfield. Registration of 3-D intraoperative MR images of the brain using a finite-element biomechanical model. *IEEE transactions on medical imaging*, 20(12):1384–97, December 2001.

[6] Nazim Haouchine, Jeremie Dequidt, Igor Peterlik, Erwan Kerrien, and Marie-Odile Berger. Image-guided simulation of heterogeneous tissue deformation for augmented reality during hepatic surgery. In *Proc. of ISMAR, Int. Symposium on Mixed and Augm. Reality*, 2013.

[7] Yipeng Hu, Hashim Uddin Ahmed, Zeike Taylor, Clare Allen, Mark Emberton, David Hawkes, and Dean Barratt. MR to ultrasound registration for image-guided prostate interventions. *Medical image analysis*, 16(3):687–703, December 2012.

[8] Tungyou Lin, Carole Le Guyader, Ivo Dinov, Paul Thompson, Arthur Toga, and Luminita Vese. A Landmark-Based Image Registration Model using a Nonlinear Elasticity Smoother for Mapping Mouse Atlas to Gene Expression Data. *Sciences-New York*, 2009.

[9] Bahram Marami, Shahin Sirouspour, and D. Capson. Model-based deformable registration of preoperative 3D to intraoperative low-resolution 3D and 2D sequences of MR images. *Medical Image Computing and Computer-Assisted Intervention–MICCAI 2011*, pages 460–467, 2011.

[10] Matthias Müller and Markus Gross. Interactive virtual materials. In *GI '04: Proc. of Graphics Interface 2004*, pages 239–246, School of Computer Science, University of Waterloo, Waterloo, Ontario, Canada, 2004. Canadian Human-Computer Communications Society.

[11] Nahyup Kang and Min Woo Lee and Taehyun Rhee. Simulating Liver Deformation during Respiration Using Sparse Local Features. *Computer Graphics and Applications*, 32(5):29–38, 2012.

[12] Karteek Popuri, Dana Cobzas, and Martin Jagerstand. Fast FEM-based non-rigid registration. In *Canadian Conference on Computer and Robot Vision*, pages 378—-385, 2010.

[13] Torsten Rohlfing, Calvin R. Maurer, Walter G. O'Dell, and Jianhui Zhong. Modeling liver motion and deformation during the respiratory cycle using intensity-based nonrigid registration of gated MR images. *Medical Physics*, 31(3):427, 2004.

[14] Szymon Rusinkiewicz and Marc Levoy. Efficient variants of the icp algorithm. In *3-D Digital Imaging and Modeling, 2001. Proceedings. Third International Conference on*, pages 145–152. IEEE, 2001.

[15] G. Saupin, C. Duriez, S. Cotin, and L. Grisoni. Efficient contact modeling using compliance warping. In *Computer Graphics International*, 2008.

[16] Alexander I. Veress, Nikhil Phatak, and Jeffrey A. Weiss. Deformable image registration with Hyperelastic Warping. *Handbook of Biomedical Image Analysis*, (Figure 1):487–533, 2005.